STUDIES

Integrating moment ratio and relative intensity methods for earthquake forecasting: a case study of the Zagros region

Meriem Benhachiche
(corresponding author)
Laboratory MSTD,
Faculty of Mathematics,
University of Science and Technology Houari-Boumediene,
Hazard and Geological Risk Division,
Algiers, Algeria
Email: benhachichemeriem@gmail.com

Nassim Hallal
Hazard and Geological Risk Division,
Algiers, Algeria
Email: n.hallal@craag.dz

Mohammad Talebi
Tehran Disaster Mitigation and Management Organisation (TDMMO),
Tehran, Iran
Email: m.talebi@iiees.ac.ir

This study examined the Zagros region by combining two earthquake forecasting methods: moment ratio (MR) and relative intensity (RI). The proposed combined moment ratio (CMR) method used a unified catalogue of earthquakes with magnitudes $M_w \geq 3.0$ that occurred during 1980–2023. The regional forecast maps with hotspots based on the results of the retrospective forecast showed the probable earthquake-prone areas with magnitudes $M_w \geq 5.5$ from 2019 to 2023. The relative (or receiver) operating characteristic and Molchan diagrams are used to evaluate the comparative performance of MR, RI and CMR approaches. The results show that the CMR method outperforms MR and RI methods.

Keywords:
earthquake forecasting,
moment ratio,
relative intensity,
combined moment ratio,
relative (or receiver) operating characteristic,
Molchan diagrams

Online first publication date: 26 August 2025

Introduction

Earthquakes are destructive natural disasters around the world. A major earthquake can cause significant fatalities and property loss. Thus, earthquake forecasting can be a useful tool to manage and reduce the seismic risk. The scientific community has been actively investigating earthquake forecasting methods. Despite significant advancements in earthquake forecasting, the field has yet to reach a stage where precise, time-specific alerts can be reliably issued to society. Current forecasting methods are based on the probabilistic assessments of seismic risks over extended periods rather than on accurate predictions of when and where an earthquake might occur. Currently, no consistent mechanism for predicting the exact time and location of the next significant earthquake exists, unlike other natural phenomena such as rainfall and storms, which might be predicted with a certain degree of precision (Rikitake 1968).

Earthquake forecasting uses approaches generally categorised as empirical and probabilistic approaches. Empirical approaches focus on abnormal phenomena (precursors) that might precede an earthquake (e.g. abnormal changes in seismic activity, ground movements, electromagnetic signals, chemical emissions and changes in animal behaviour). In contrast, probabilistic approaches rely on statistical models that analyse seismicity patterns using quantitative data. Despite the reasonable skill and reliability of both methods, earthquake forecasting remains an open field, even as scientific interest is continuously growing (Jordan 2006, Jordan–Jones 2010). Currently, statistical seismicity models – developed to evaluate the likelihood of future earthquakes within a specific time–space–magnitude window – form the primary basis for earthquake forecasting (Holliday et al. 2005, Ghaedi–Ibrahim 2017, Mojarab et al. 2015, Nanjo et al. 2006, Peresan et al. 2005, Ogata 2011, Rundle et al. 2003, Peresan–Romashkova 2022, Tiampo–Shcherbakov 2013, Radan et al. 2013).

The primary challenge lies in the fact that success probability rates derived from statistical seismicity models are not always significant for use in operational forecasting, which demands high forecasted earthquake rates to support critical decisions such as evacuations or other emergency responses (Jordan–Jones 2010). One potential solution is to combine multiple methods, which might enhance forecasting capabilities. However, integrating diverse forecasting approaches remains a significant challenge in seismic risk mitigation and management. Considering the non-linear and multi-scale nature of earthquake processes, effective forecasting requires a synthesis of statistical, physical and machine learning techniques, as reported by Jordan et al. (2011). Various approaches to improve earthquake forecasting through model combination have been reported (Rhoades–Gerstenberger 2009). To improve forecasting accuracy, Shebalin et al. (2014) combined earthquake forecasts using differential probability gains. Similarly, to improve the seismic hazard assessment of the Central China North–South Seismic Belt, Zhang et al. (2022) integrated the pattern informatics (PI) method with its modified version (PIm), which

incorporated earthquake magnitude instead of earthquake occurrence count statistics. Furthermore, Zhang et al. (2024) introduced a successful new approach that integrated deep learning techniques with the epidemic-type aftershock sequence benchmark seismicity model to forecast earthquake events.

This study improves earthquake forecasting for Zagros by combining two statistical approaches: the moment ratio (MR) and relative intensity (RI). The MR approach is based on the statistical analysis of earthquake inter-event times. It uses the ratio of the first- and second-order moments of earthquake inter-event times as a forecasting index to monitor impending seismicity. It successfully forecasted large earthquakes in Japan across short-, medium- and long-term periods (Talbi et al. 2013), and was tested in regions of moderate seismicity such as Turkey (Talbi et al. 2019). This study incorporated relatively low-magnitude events ($M_w \geq 4.5$) to forecast high-magnitude events ($M_w \geq 5.5$), thereby improving statistical estimates through dense space–time coverage of the testing zone. However, to demonstrate its effectiveness, the MR method must be evaluated on a global scale, similar to other forecasting strategies. Testing it across various regions is essential to generalize its worldwide applicability. Beyond enhancing its evaluation, certain issues related to its implementation and processing should be addressed. Thus, the present analysis aims to generalize the MR applicability to countries with different tectonic settings, as demonstrated through its application to seismicity in the Zagros region. The RI method is a statistical forecasting approach that estimates earthquake probabilities based on the spatial distribution of past earthquakes. It assumes that regions with a high density of past earthquakes are highly susceptible to experiencing future earthquakes (Holliday et al. 2005). It has been tested in various global regions with varying degrees of success (Chen et al. 2006, Jiang–Wu 2011, Nanjo 2011, Cho–Tiampo 2013, Chang et al. 2016, Zhang et al. 2018). Practically, combining methods involves integrating multiple seismicity models using an objective function. This study introduces a combined forecasting method, referred to as the combined moment ratio (CMR), which integrates the MR and RI approaches. The CMR index is derived by summing the normalised MR and RI indices, thereby integrating spatial and temporal insights to enhance forecasting performance.

Earthquakes in the Zagros region are concentrated along a highly tectonically active zone formed by the collision of two major plates: the continental Arabian plate and the continental microplate of Central Iran. Zagros is an earthquake-prone region of the Iranian plateau with relatively high seismicity. Thus, a natural laboratory for testing forecasting methods is situated in Zagros. These factors, among others, motivated the seismicity analysis conducted in this study. Notably, in recent years, the Zagros region has been the focus of numerous studies using different approaches (Naderzadeh–Madani 2012, Shishegaran et al. 2019, Ommi–Hashemi 2024).

This study improved the MR and RI forecasting approaches, by proposing a combined method (CMR) and studied seismicity in the Zagros region. MR, RI and

CMR models were used to forecast target earthquakes with magnitudes $M_w \geq 5.5$, while accounting for the completeness of magnitude data used during the learning and forecasting phases. The training periods commenced from the first year in which magnitude completeness was achieved for a given threshold. This choice is optimal, as it ensured access to the largest and most accurate available database, filtered according to the estimated magnitude of completeness (Talbi et al. 2019). The obtained results are presented as earthquake forecasting maps for target earthquakes with magnitudes exceeding or equal to M_w 5.5. Hotspots with expected high probabilities of target earthquakes are high-alarm areas. The forecasting performance of these methods was evaluated using the relative (or receiver) operating characteristic (ROC) (Jolliffe–Stephenson 2003) and Molchan error diagrams (Molchan 1997, 2003, 2010), which enabled comparison of the results with those derived using a random guessing strategy or a reference method. The ROC diagram graphically represents the hit rate *(h)* against the false alarm rate *(f)*. In contrast, the Molchan diagram graphically represents the failure rate *(ν)* versus the space–time alarm rate (τ), which represents the fraction of space–time under alarm. The CMR forecast results presented in this study demonstrated good performance, outperforming the random guessing strategy and the individual MR and RI methods.

Earthquake database

The Zagros region covers the spatial window situated between 22° N and 42° N latitude and 41° E and 66° E longitude (see in Appendix Figure A1). This region is a relatively highly seismically active tectonic province of the Iranian plateau. Continuous collision between the continental Arabian plate and the continental microplate of Central Iran since the Miocene has resulted in the formation of the NW-trending Zagros fold-and-thrust belt (Alavi 1994, Agard et al. 2005, Mouthereau et al. 2012). Crustal shortening, thrusting and folding in Zagros accommodate approximately half of the convergence between the Arabian and Eurasian plates (e.g. Vernant et al. 2004). Over time, the area has experienced numerous strong and destructive earthquakes: the 1853 Shiraz earthquake (M_s 6.2), 13,000 casualties; the 1909 Silakhur earthquake (M_s 7.4), 5,500 casualties; the 1957 Farsinaj earthquake (M_s 6.7), 1,200 fatalities; and the 1972 Qir earthquake (M_s 6.9), extensive damage and ~30,000 casualties. The 2017 M_w 7.4 Sarpol Zahab earthquake in the Kermanshah Iranian province, close to the Iran–Iraq border, is the most recent major earthquake in the Zagros region with ~620 casualties (Ambraseys–Melville 1982, Raeesi et al. 2017, Saleh et al. 2023).

Zagros experiences widespread seismic activity of different magnitudes (usually $< M \approx 7$) (Talebian–Jackson 2004). The instrumental seismicity of the Iranian plateau has been reported in several regional and global catalogues. Three main periods can be identified in relation to the development of local seismic networks in

Iran, each characterised by differing levels of data accuracy: (i) 1900–1964 and (ii) 1964–1996 corresponding to the periods after the global-scale installation of modern seismological instruments, which concluded in 1996 – and (iii) the post-1996 period, corresponding to the development of local seismic networks within Iran. Therefore, the earthquake parameter uncertainty values decreased with time, particularly resulting from network improvements.

This study uses the earthquake catalogue compiled by Mousavi-Bafrouei and Mahani (2020), which includes events with magnitudes of $M_w \geq 3.0$, hereafter referred to as MB2020. MB2020 remains the most recent catalogue available for the Zagros region. However, the most recent instrumental portion of MB2020 is primarily sourced from seismic data provided by the Iranian Seismological Centre (IGUT). Since MB2020 covers data only up to 2019, the IGUT catalogue was used to extend it by incorporating recent data from 2019 to 2023. Additionally, the same regression relation used in MB2020 was used to harmonise the magnitude scale of the extended catalogue. The resulting earthquake catalogue data file included events with magnitudes listed on the moment–magnitude scale (M_w).

A key parameter in any seismicity study based on an earthquake catalogue is the completeness magnitude (M_c), which should be systematically estimated to ensure statistical consistency. This parameter represents the minimum magnitude above which earthquakes are assumed to be completely reported in the earthquake data file. Herein, the goodness-of-fit method (Mignan–Woessner 2012) was applied to estimate M_c, which was 4.5 starting from 1996. Figure A1 (see in Appendix) shows the spatial distribution of earthquake epicentres with magnitudes exceeding M_c from 1996 to 2023.

MR and RI forecasting indices

The MR approach, an alarm-based method for earthquake forecasting, uses the ratio of the first- and second-order moments of earthquake inter-event times as an alarm index. This method assumes that the MR forecasting index is associated with anomalous long-term changes in background seismicity before large earthquakes (Talbi et al. 2013). An earthquake catalogue prepared for a specific region *G* over a specified period serves as a primary input for estimating the MR index in each cell and constructing forecasting maps. The study region *G* is divided into grid cells of the same size ($l \times l$), as shown in Figure 1, where l is linked to the rupture size of target earthquakes.

Figure 1

Schematic diagram illustrating the neighbouring cells surrounding cell *i* used collectively in sampling

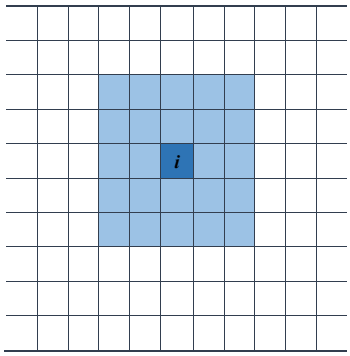

Two distinct periods are considered: (a) a learning period, spanning from t_0 to t_1 ($t_0 < t_1$), where t_0 is the initial time of the analysis and (b) a testing period from t_1 to t_2 ($t_1 < t_2$), during which the forecast is evaluated. A schematic diagram illustrating these periods is shown in Figure 2.

Figure 2

Schematic diagram illustrating the time intervals used in MR and RI learning and testing phases

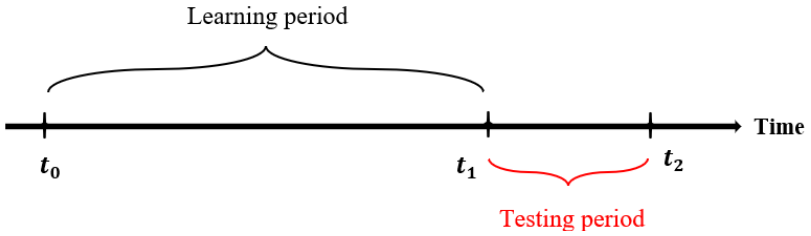

The MR index for each cell $i \in G$ is defined as the ratio of the mean inter-event time series $\{\xi_i\}_{i=1:n}$ to the variance calculated during the learning period $[t_0, t_1[$. This index serves as a precursory alarm function for forecasting future earthquakes with magnitudes $M \geq M_t$ – referred to as target magnitudes during the forecasting period $[t_1, t_2]$. The MR statistic is expressed as equation (1).

$$MR_i(t_0, t_1) = \frac{\bar{\xi}_i}{{\sigma_\xi}^2}, \quad i = 1{:}\, n \tag{1}$$

where $\bar{\xi}_i$ and ${\sigma_\xi}^2$ represent the arithmetic mean and variance, respectively, of the inter-event time series$\{\xi_i\}_{i=1:n}$. Subsequently, the standardised MR alarm function, MR_i, for each cell $i \in G$, is defined using equation (2).

$$MR_i = \frac{MR_i}{max_{i \in G}(MR_i)} \tag{2}$$

The RI method was initially introduced by Holliday et al. 2005. It is based on the hypothesis that significant target earthquakes are highly probable to occur in spatial locations that have historically experienced high seismic activity (Tiampo–Sherbakov 2012). Accordingly, the RI index is defined as the estimated frequency of past earthquakes. In practice, earthquake statistics from $[t_0, t_1[$, are used to forecast target earthquakes with magnitudes $M \geq M_t$ during $[t_1, t_2]$. For each cell i, the RI index is defined as the total number of learning-period earthquakes with $M \geq M_c$, $n_i(t_0, t_1)$, divided by the total number of such earthquakes across the entire study region G using equation (3).

$$RI_i(t_0, t_1) = \frac{n_i(t_0,t_1)}{\sum_{i=1}^{n} n_i(t_0,t_1)} \quad (3)$$

Similarly, the standardised RI alarm function, RI_i, for each cell $i \in G$ is defined using equation (4).

$$RI_i = \frac{RI_i}{max_{i \in G}(RI_i)} \quad (4)$$

To improve the performance of the MR method, this study introduces CMR that integrates MR and RI methods by summing their respective indices. For each cell i, the CMR is defined using equation (5).

$$CMR_i = MR_i + RI_i \quad (5)$$

The CMR index is normalised by its maximum value across all cells in the study region similar to equations (2) and (4), as shown in equation (6).

$$CMR_i = \frac{CMR_i}{max_{i \in G}(CMR_i)} \quad (6)$$

The results of the application of the former methods to Zagros seismicity are presented as forecast maps showing hotspot areas where large earthquakes are expected to occur during $[t_1, t_2]$. To ensure significant statistics, these methods are used in the active cells with a minimum number of earthquakes $n \geq n_{min}$ that occurred during $[t_0, t_1[$. This criterion is used to maintain the stability of the results and guarantee an acceptable degree of accuracy of our estimates.

Forecasting evaluation

Two widely accepted statistical tools commonly used to evaluate the performance of earthquake forecasting methods are the ROC diagram (Jolliffe–Stephenson 2003, Holliday et al. 2005), and the Molchan diagram (Molchan 1997, 2003, 2010).

The ROC diagram for an alarm-based model is a plot of the false alarm rate f (on the x-axis), which shows the percentage of alarms that do not forecast earthquakes, versus the hit rate h (on the y-axis), which shows the proportion of earthquakes that are successfully forecasted. These parameters are expressed in equation (7).

$$h = \frac{a}{a+c}, f = \frac{b}{b+d} \quad (7)$$

There are four possibilities of earthquake occurrences during $[t_1, t_2]$.

1. An earthquake occurs in one alarmed cell (an alarm cell is a cell with an index exceeding a given threshold, $I_i \geq C_0$)(success). The number of such cells is *a*.
2. No earthquake occurs in a non-alarmed cell ($I_i < C_0$)(success). The number of such cells is *d*.
3. No earthquake occurs in an alarmed cell (false alarm). The number of such cells is *b*.
4. An earthquake occurs in a non-alarm cell (failure to forecast). The number of such cells is *c*.

The Molchan error diagram plots the failure to forecast rate ν – defined as the number of unforecasted earthquakes divided by the total number of occurred earthquakes – against the space–time alarm rate τ, which represents the ratio of alarmed cells to the total number of cells in the study area and is expressed as equation (8).

$$\nu = \frac{c}{a+c}, \tau = \frac{a+b}{a+b+c+d} \tag{8}$$

For a given space–time region, the alarm-based model is entirely characterised by its alarm function, denoted $A \in [0,1]$. When $A \in [0,1]$ exceeds a given threshold value, say C_0, an alarm is issued and a target earthquake is forecasted. The C_0 values are ordered from the smallest to the largest. Additionally, a diagonal line is plotted on the ROC diagram from the lower-left corner to the upper-right corner, representing a random forecast, and is identified by the equation $b = f$. Effective forecasting performance is indicated when the curve lies above the diagonal reference line. In contrast, the diagonal line in the Molchan diagram extending from the upper left corner to the lower right corner represents the performance of a random forecast. A forecasting method performs well when the graph is below this diagonal.

Moreover, the binomial distribution of the number of chance hits within the alarm region can be used to construct confidence intervals for the Molchan diagram (Kossobokov 2006, Zechar–Jordan 2008). Within this framework, the curve Γ_α, corresponding to a confidence level of $1 - a$, is defined using equations (9) and (10).

$$\Gamma_\alpha = \{(\tau, \nu_a(\tau)) \in [0, 1] \times \{1, 2, \ldots, N\}\} \tag{9}$$

$$\nu_\alpha(\tau) = 1 - [\min_{1 \leq k \leq N} \{k/P(\boldsymbol{\mathcal{B}}(N, \tau) = k - 1) > 1 - a\}/N] \tag{10}$$

where N represents the number of target events that occurred within the testing region G, and k denotes the number of successful hits.

Application and results

The Zagros region, known for its relatively high seismic activity, has been selected as the study area to demonstrate the results of various earthquake forecasting approaches for events with magnitudes $M \geq M_t$, where $M_t = 5.5$ (Table 1). This magnitude class is called the target magnitude. The results are presented as forecasting maps constructed using optimal parameters obtained from a retrospective analysis of

the unified earthquake catalogue compiled earlier. One crucial parameter is the cell size, which plays a key role in earthquake forecasting owing to its relation with rupture areas potentially spanning multiple cell sizes. Large cell sizes can enhance forecasting performance by covering a wide area and increasing the overall hit rate. However, large cell sizes might reduce forecasting precision, as they encompass broad geographical regions, making it hard to localise forecasts.

The MR method was performed using the mentioned parameters: (i) a cell size, l = 0.25° suitable for forecasting earthquakes with magnitudes $M \geq 5.5$, (ii) $[t_0, t_1[$ = [1996, 2019[, and (iii) $[t_1, t_2]$= [2019, 2023]. Thus, 1,804 earthquakes with magnitudes $M \geqslant 4.5$ occurring in Zagros were used during $[t_0, t_1[$. The next step removing non-Poissonian (dependent) earthquakes (foreshocks, aftershocks and swarms) – to ensure that the forecasting b is not artificially inflated by aftershock occurrences, especially in the case of a successful major event forecast. To accomplish this, Gardner and Knopoff's (1974) method is used to produce a declustered catalogue using Zmap software (Wiemer 2001). Table 1 presents 14 background events obtained after declustering the catalogue in the testing zone during the considered testing period with target magnitudes of $M \geq 5.5$.

Table 1

List of target earthquakes with magnitudes $M \geq 5.5$ that occurred in the testing region during 2019–2023

N	Longitude (°E)	Latitude (°N)	Date	Time	Magnitude
1	49.55	31.89	08/07/2019	07:00	5.8
2	54.99	27.07	21/10/2019	10:58	5.7
3	52.09	29.61	27/01/2020	13:28	5.5
4	55.85	26.98	16/02/2020	12:30	5.9
5	57.28	28.30	27/03/2020	06:40	5.5
6	53.35	27.67	09/06/2020	16:08	5.5
7	53.43	27.63	09/06/2020	17:18	5.8
8	55.29	26.71	15/01/2021	21:31	5.5
9	50.67	29.73	18/04/2021	06:41	6.0
10	49.75	32.33	04/10/2021	02:39	5.9
11	56.17	27.54	14/11/2021	12:08	6.4
12	54.65	26.89	16/03/2022	23:15	5.9
13	55.30	26.84	01/07/2022	21:32	6.2
14	55.39	26.80	23/07/2022	16:09	5.8

Herein, the MR, RI and CMR methods use the neighbouring cells surrounding each cell i, as shown in Figure 1, for the computation of statistics $\bar{\xi}_i$ and $n_i(t_0, t_1)$. This integration increases the number of cells in the testing region and forecasting performance. Furthermore, checking different values for the minimum sample size n_{min} indicates the n_{min} value of 20 to optimally reduce alert rates, guaranteeing accuracy and preserving result stability. Consequently, MR and RI indices estimated by considering at least 20 inter-event times or number of events are considered in our

calculation ($n \geq 20$). Or else, the cell is disregarded and labelled as empty or assigned no estimate, it is excluded from analysis. To ensure a fair comparison, the RI method is used applying the same parameters and conditions. Finally, the CMR strategy is implemented. The resulting forecasting maps for these methods are illustrated using coloured cells, highlighting hotspot regions (see in Appendix Figures A2, A3 and A4). Figure A2 shows the MR forecasting map for Zagros, highlighting target-magnitude events that occurred during 2019–2023. MR indices are estimated according to the colour-coded legend. Similarly, Figure A3 shows the RI forecasting map for the same region and testing period. Figure A4 shows the forecasting results obtained using our proposed CMR approach. The map illustrates the previously identified target events with magnitudes $M \geq 5.5$, and the colour scale represents the CMR indices. Additionally, all maps display target earthquakes with $M \geq 5.5$, marked by black circles. The total number of space–time cells is given by multiplying the number of space cells by the number of time steps. For this test, we consider a one-time step (Δt), resulting in 632 space–time cells (a testing region).

Finally, the obtained results are tested using ROC and Molchan diagrams. These diagrams rely on systematically varying the alarm threshold C. The values a (forecast = yes, observed = yes), b (forecast = yes, observed = no), c (forecast = no, observed = yes) and d (forecast = no, observed = no) were estimated. In Appendix Figures A5a and A5b show the evaluation of each forecasting method – MR (red curve), RI (blue curve) and CMR (black curve) – using the ROC and corresponding Molchan diagrams, respectively. The diagonal lines in Figures A5a and A5b represent the performance of a random forecast, with a confidence interval α of 5%. Both diagrams indicate that the CMR approach outperforms the other two methods.

Discussion and conclusion

This study enhanced earthquake forecasting methods. However, it is crucial to emphasise that all proposed approaches have failed to provide precise, time-specific warnings to date. The proposed forecasting method is a probabilistic approach capable of identifying regions where future earthquakes are expected over extended periods. Nonetheless, the method does not offer real-time alerts or enable precise predictions regarding the exact timing and location of future seismic events.

To improve earthquake forecasting in Zagros, this study used the CMR method by combining MR and RI methods. The complementary strengths of MR and RI methods improved the CMR method. While RI efficiently displayed spatial regions with historically high seismic activity, the MR approach resumed inter-event time patterns to identify time anomalies. A forecasting model is proposed that combines these indices using a straightforward summarisation technique, leveraging the strengths of each index. By combining these methods, the CMR approach linked temporal and spatial dimensions and patterns of earthquake precursors, providing a

complete forecasting approach. Our analysis demonstrated that the inherent limitations of individual models could be mitigated by integrating multiple forecasting techniques. The retrospective testing conducted in this study showed the good performance of the CMR method compared to individual MR and RI models using ROC and Molchan diagrams. The CMR method outperformed random guessing and the MR and RI methods, effectively identifying seismic hotspots with an elevated risk of earthquakes with magnitudes $M \geq 5.5$.

MR and RI methods were selected for the combination based on their robustness, successful across different regions and complementary characteristics. Although numerous forecasting techniques are available, the simplicity and interpretability of MR and RI were ideal for integration. Moreover, the summation-based approach retained the intuitive nature of the indices while significantly enhancing performance.

Future research should aim to refine the CMR method by exploring adaptive weighting strategies for combining indices, optimising spatial resolution and potentially incorporating additional forecasting models. Reducing false alarm rates remains a critical challenge, which can be addressed through enhanced parameter selection and machine learning integration. Additionally, future studies should involve testing the CMR method in other tectonically active regions to evaluate its generalisability and adaptability to diverse seismic settings. The CMR method offers valuable and significant insights for seismic forecasting. The application of this method to Zagros yielded promising results and established a foundation for evaluating its applicability in other areas.

Acknowledgement

We are grateful to Abdelhak Talbi for his help and advice in revising this manuscript.

Appendix

Figure A1

Spatial distribution of earthquakes with magnitudes above M_c in Zagros from 1996 to 2023

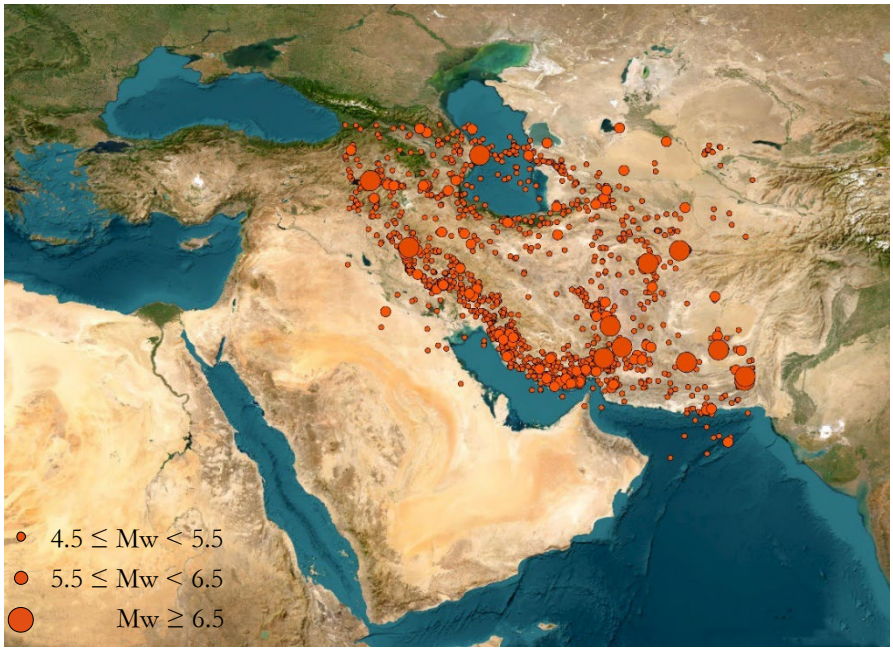

Figure A2

MR forecasting map for Zagros showing target earthquakes with $M \geq 5.5$ that occurred during 2019–2023

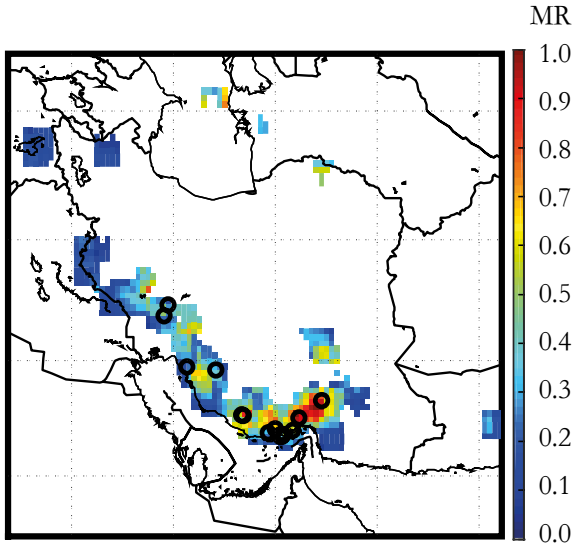

Figure A3

RI forecasting map for Zagros showing target earthquakes with $M \geq 5.5$ that occurred during 2019–2023

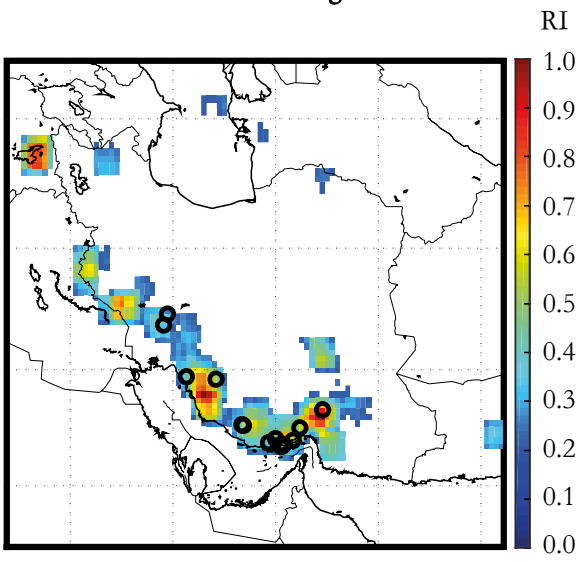

Figure A4

CMR forecasting map for Zagros showing target earthquakes with $M \geq 5.5$ that occurred during 2019–2023

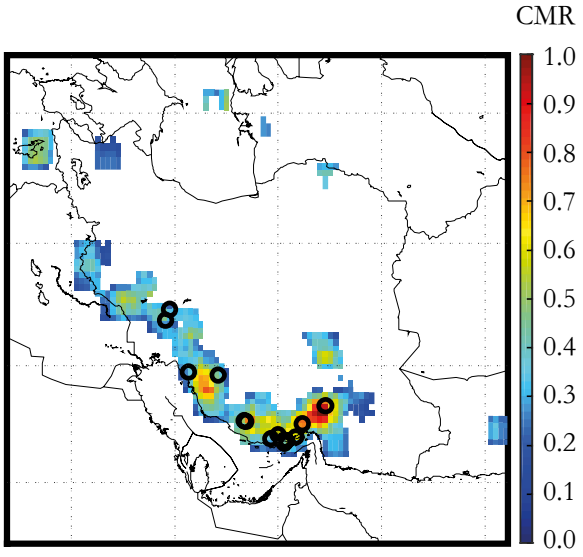

Figure A5

ROC and Molchan diagrams for target earthquakes with $M \geq 5.5$ in Zagros during 2019–2023

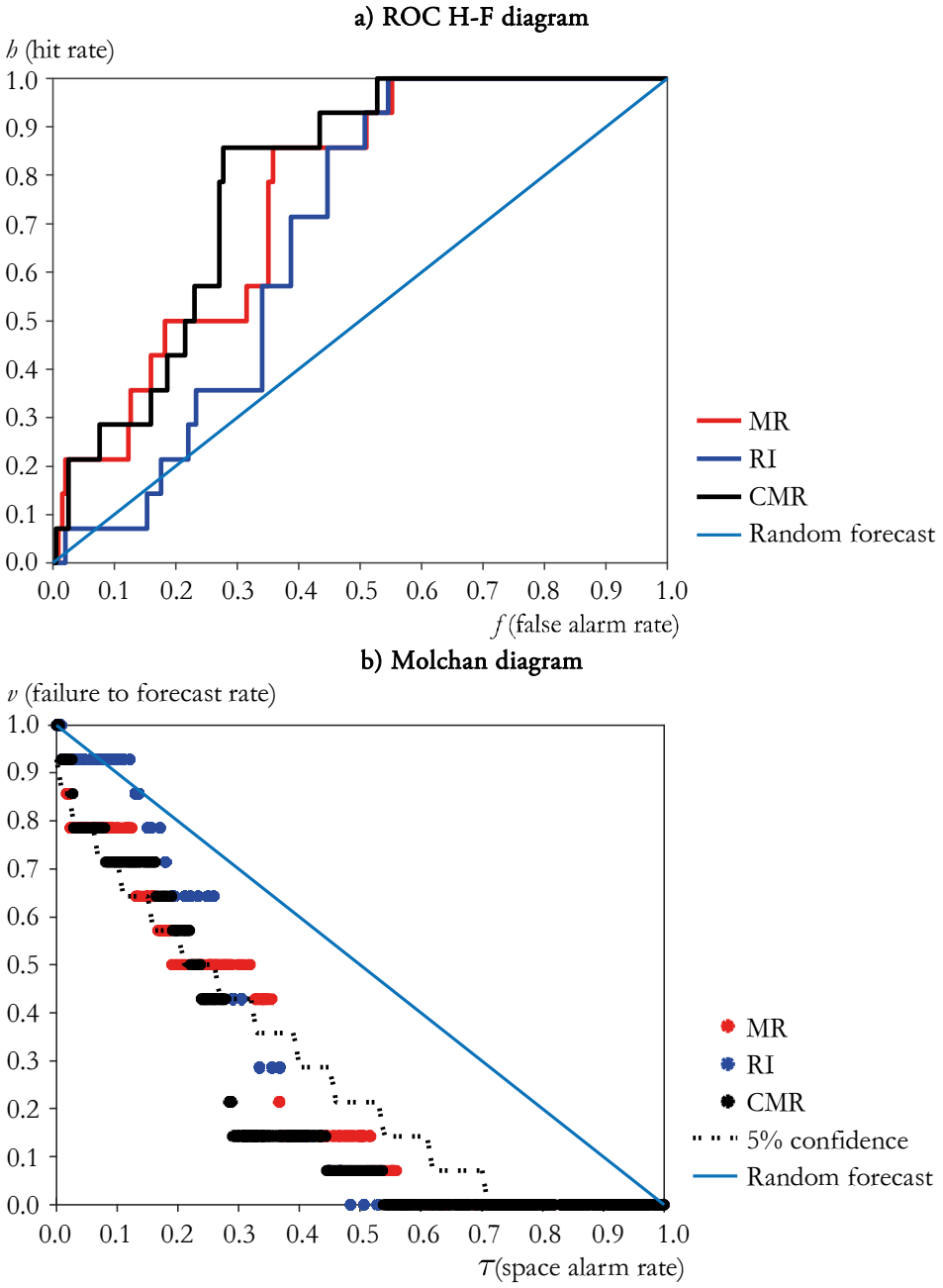

REFERENCES

AGARD, P.–OMRANI, J.–JOLIVET, L.–MOUTHEREAU, F. (2005): Convergence history across Zagros (Iran): constraints from collisional and earlier deformation *International Journal of Earth Sciences* 94: 401–419. https://doi.org/10.1007/s00531-005-0481-4

ALAVI, M. (1994): Tectonics of the Zagros orogenic belt of Iran: new data and interpretations *Tectonophysics* 229 (3–4): 211–238. https://doi.org/10.1016/0040-1951(94)90030-2

AMBRASEYS, N.–MELVILLE, C. (1982): *A history of Persian earthquakes* Cambridge University Press, Cambridge.

CHANG, L. Y.–CHEN, C. C.–WU, Y. H.–LIN, T. W.–CHANG, C. H.–KAN, C. W. (2016): A strategy for a routine pattern informatics operation applied to Taiwan *Pure and Applied Geophysics* 173: 235–244. https://doi.org/10.1007/s00024-015-1079-9

CHEN, C. C.–RUNDLE, J. B.–HSIEN-CHI, L.–HOLLIDAY, J. R.–NANJO, K. Z.–TURCOTTE, D. L.–TIAMPO, K. F. (2006): From tornadoes to earthquakes: forecast verification for binary events applied to the 1999 Chi-Chi, Taiwan, earthquake *TAO: Terrestrial, Atmospheric and Oceanic Sciences* 17 (3): 503. https://doi.org/10.3319/TAO.2006.17.3.503(T)

CHO, N. F.–TIAMPO, K. F. (2013): Effects of location errors in pattern informatics *Pure and Applied Geophysics* 170: 185–196. https://doi.org/10.1007/s00024-011-0448-2

GARDNER, J. K.–KNOPOFF, L. (1974). Is the sequence of earthquakes in Southern California, with aftershocks removed, Poissonian? *Bulletin of the seismological society of America* 64 (5): 1363–1367. https://doi.org/10.1785/BSSA0640051363

GHAEDI, K.–IBRAHIM, Z. (2017): Earthquake prediction *Earthquakes-Tectonics, Hazard and Risk Mitigation* 66: 205–227. https://doi.org/10.5772/65511

HOLLIDAY, J. R.–NANJO, K. Z.–TIAMPO, K. F.–RUNDLE, J. B.–TURCOTTE, D. L. (2005): Earthquake forecasting and its verification *Nonlinear Processes in Geophysics* 12 (6): 965–977. https://doi.org/10.5194/npg-12-965-2005

JIANG, C. S.–WU, Z. L. (2011): PI forecast with or without de-clustering:an experiment for the Sichuan-Yunnan region *Natural Hazards and Earth System Sciences* 1 (3): 697–706. https://doi.org/10.5194/nhess-11-697-20

JOLLIFFE, L. T.–STEPHENSON, D. B. (eds.) (2003): *Forecast verification: a practitioner's guide in atmospheric science* Wiley, Hoboken.

JORDAN, T. H. (2006): Earthquake predictability, brick by brick *Seismological Research Letters* 77 (1): 3–6. https://doi.org/10.1785/gssrl.77.1.3

JORDAN, T. H.–CHEN, Y. T.–GASPARINI, P.–MADARIAGA, R.–MAIN, I.–MARZOCCHI, W.–ZSCHAU, J. (2011): Operational earthquake forecasting: state of knowledge and guidelines for utilization *Annals of Geophysics* 54 (4): 315–391. https://doi.org/10.4401/ag-5350

JORDAN, T. H.–JONES, L. M. (2010): Operational earthquake forecasting: some thoughts on why and how. *Seismological Research Letters* 81 (4): 571–574. https://doi.org/10.1785/gssrl.81.4.571

KOSSOBOKOV, V. G. (2006): Testing earthquake prediction methods: "the West Pacific short-term forecast of earthquakes with magnitude MwHRV ⩾ 5.8" *Tectonophysics* 413 (1–2): 25–31. https://doi.org/10.1016/j.tecto.2005.10.006

MIGNAN, A.–WOESSNER, J. (2012): Estimating the magnitude of completeness for earthquake catalogs *Community online resource for statistical seismicity analysis.* https://doi.org/10.5078/corssa-00180805

MOJARAB, M.–KOSSOBOKOV, V.–MEMARIAN, H.–ZARE, M. (2015): An application of earthquake prediction algorithm M8 in eastern Anatolia at the approach of the 2011 Van earthquake *Journal of Earth System Science* 124: 1047–1062. https://doi.org/10.1007/s12040-015-0584-7

MOLCHAN, G. (2010): Space–time earthquake prediction: The error diagrams. In: SAVAGE, M. K.–RHOADES, D. A.–SMITH, E. G. C.–GERSTENBERGER, M. C.–VERE-JONES, D. (eds.): *Seismogenesis and earthquake forecasting: the Frank Evison Volume II.* Pageoph Topical Volumes pp. 53–63., Springer, Basel. https://doi.org/10.1007/978-3-0346-0500-7_5

MOLCHAN, G. M. (1997): Earthquake prediction as a decision-making problem *Pure and Applied Geophysics* 149: 233–247. https://doi.org/10.1007/BF00945169

MOLCHAN, G. M. (2003): Earthquake prediction strategies: a theoretical analysis. In: KEILIS-BOROK, V. I.–SOLOVIEV, A. A. (eds.): *Nonlinear dynamics of the lithosphere and earthquake prediction* pp. 209–237., Springer Series in Synergetics, Berlin, Heidelberg. https://doi.org/10.1007/978-3-662-05298-3_5

MOUSAVI-BAFROUEI, S. H.–MAHANI, A. B. (2020): A comprehensive earthquake catalogue for the Iranian Plateau (400 BC to December 31, 2018) *Journal of Seismology* 24 (3): 709–724. https://doi.org/10.1007/s10950-020-09923-6

MOUTHEREAU, F.–LACOMBE, O.–VERGÉS, J. (2012): Building the Zagros collisional orogen: timing, strain distribution and the dynamics of Arabia/Eurasia plate convergence *Tectonophysics* 532–535: 27–60. https://doi.org/10.1016/j.tecto.2012.01.022

NANJO, K. Z. (2011): Earthquake forecasts for the CSEP Japan experiment based on the RI algorithm *Earth, Planets and Space* 63: 261–274. https://doi.org/10.5047/eps.2011.01.001

NANJO, K. Z.–HOLLIDAY, J. R.–CHEN, C. C.–RUNDLE, J. B.–TURCOTTE, D. L. (2006): Application of a modified pattern informatics method to forecasting the locations of future large earthquakes in the central Japan *Tectonophysics* 424 (3–4): 351–366. https://doi.org/10.1016/j.tecto.2006.03.043

OGATA, Y. (2011): Significant improvements of the space-time ETAS model for forecasting of accurate baseline seismicity *Earth, Planets and Space* 63: 217–229. https://doi.org/10.5047/eps.2010.09.001

OMMI, S.–HASHEMI, M. (2024): Machine learning technique in the North Zagros earthquake prediction *Applied Computing and Geosciences* 22: 100163. https://doi.org/10.1016/j.acags.2024.100163

PERESAN, A.–KOSSOBOKOV, V.–ROMASHKOVA, L.–PANZA, G. F. (2005): Intermediate-term middle-range earthquake predictions in Italy: a review *Earth-Science Reviews* 69 (1–2): 97–132. https://doi.org/10.1016/j.earscirev.2004.07.005

PERESAN, A.–ROMASHKOVA, L. (2022): Earthquake forecasting and time-dependent neo-deterministic seismic hazard assessment in Italy and surroundings. In: PANZA, G. F.–KOSSOBOKOV, V. G.–LAOR, E.–DE VIVO, B. (eds.): *Earthquakes and sustainable infrastructure* pp. 151–173., Elsevier. https://doi.org/10.1016/B978-0-12-823503-4.00007-5

RADAN, M. Y.–HAMZEHLOO, H.–PERESAN, A.–ZARE, M.–ZAFARANI, H. (2013): Assessing performances of pattern informatics method: a retrospective analysis for Iran and Italy *Natural Hazards* 68: 855–881. https://doi.org/10.1007/s11069-013-0660-8

RAEESI, M.–ZARIFI, Z.–NILFOUROUSHAN, F.–BOROUJENI, S. A.–TIAMPO, K. (2017): Quantitative analysis of seismicity in Iran *Pure and Applied Geophysics* 174: 793–833. https://doi.org/10.1007/s00024-016-1435-4

RHOADES, D. A.–GERSTENBERGER, M. C. (2009): Mixture models for improved short-term earthquake forecasting *Bulletin of the Seismological Society of America* 99 (2A): 636–646. https://doi.org/10.1785/0120080063

RIKITAKE, T. (1968): Earthquake prediction *Earth-Science Reviews* 4: 245–282. https://doi.org/10.1016/0012-8252(76)90076-3

RUNDLE, J. B.–TURCOTTE, D. L.–SHCHERBAKOV, R.–KLEIN, W.–SAMMIS, C. (2003): Statistical physics approach to understanding the multiscale dynamics of earthquake fault systems *Reviews of Geophysics* 41: 1019–1038. https://doi.org/10.1029/2003RG000135

SALEH, M.–MEGHRAOUI, M.–ÇETIN, E. (2023): The 12 November 2017 Mw 7.4 earthquake in Sarpol-e-Zahab (Iran–Iraq): a complex fault rupture in the Zagros Mountains *Mediterranean Geoscience Reviews* 5 (3): 177–188. https://doi.org/10.1007/s42990-023-00107-1

SHEBALIN, P. N.–NARTEAU, C.–ZECHAR, J. D.–HOLSCHNEIDER, M. (2014): Combining earthquake forecasts using differential probability gains *Earth, Planets and Space* 66: 34. https://doi.org/10.1186/1880-5981-66-37

SHISHEGARAN, A.–TAGHAVIZADE, H.–BIGDELI, A.–SHISHEGARAN, A. (2019): Predicting the earthquake magnitude along Zagros fault using time series and ensemble model *Journal of Soft Computing in Civil Engineering* 3 (4): 67–77. https://doi.org/10.22115/scce.2020.213197.1152

TALBI, A.–BELLALEM, F.–MOBARKI, M. (2019): Turkey and adjacent area seismicity forecasts from earthquake inter-event time mean ratio statistics *Journal of Seismology* 23 (3): 441–453. https://doi.org/10.1007/s10950-019-09816-3

TALBI, A.–NANJO, K.–ZHUANG, J.–SATAKE, K.–HAMDACHE, M. (2013): Interevent times in a new alarm-based earthquake forecasting model *Geophysical Journal International* 194 (3): 1823–1835. https://doi.org/10.1093/gji/ggt194

TALEBIAN, M.–JACKSON, J. (2004): A reappraisal of earthquake focal mechanisms and active shortening in the Zagros mountains of Iran *Geophysical Journal International* 156 (3): 506–526. https://doi.org/10.1111/j.1365-246X.2004.02092.x

TIAMPO, K. F.–SHCHERBAKOV, R. (2012): Seismicity-based earthquake forecasting techniques: ten years of progress *Tectonophysics* 522–523: 89–121. https://doi.org/10.1016/j.tecto.2011.08.019

TIAMPO, K. F.–SHCHERBAKOV, R. (2013): Optimization of seismicity-based forecasts *Pure and Applied Geophysics* 170: 139–154. https://doi.org/10.1007/s00024-012-0457-9

VERNANT, P.–NILFOROUSHAN, F.–HATZFELD, D.–ABBASSI, M. R.–VIGNY, C.–MASSON, F.–NANKALI, H.–MARTINOD, J.–ASHTIANI, A.–BAYER, R.–TAVAKOLI, F.–CHERY, J. (2004): Present-day crustal deformation and plate kinematics in the Middle East constrained by GPS measurements in Iran and northern Oman *Geophysical Journal International* 157 (1): 381–398. https://doi.org/10.1111/j.1365-246X.2004.02222.x

WIEMER, S. (2001): A software package to analyze seismicity: ZMAP *Seismological Research Letters* 72 (3): 373–382. http://dx.doi.org/10.1785/gssrl.72.3.373

ZECHAR, J. D.–JORDAN, T. H. (2008): Testing alarm-based earthquake predictions *Geophysical Journal International* 172 (2): 715–724. https://doi.org/10.1111/j.1365-246X.2007.03676.x

ZHANG, H.–KE, S.–LIU, W.–ZHANG, Y. (2024): A combining earthquake forecasting model between deep learning and epidemic-type aftershock sequence (ETAS) model *Geophysical Journal International* 239 (3): 1545–1556. https://doi.org/10.1093/gji/ggae349

ZHANG, S.–WU, Z.–ZHANG, Y. (2022): Pattern informatics (PI) of seismicity considering earthquake magnitude? An experiment in the Central China north–south seismic belt *Pure and Applied Geophysics* 179: 4095–4102. https://doi.org/10.1007/s00024-022-03079-9

ZHANG, Y.–XIA, C.–SONG, C.–ZHANG, X.–WU, Y.–XUE, Y. (2018): Test of the predictability of the PI method for recent large earthquakes in and near Tibetan Plateau. In: ZHANG, Y.–GOEBEL, T.–PENG, Z.–WILLIAMS, C.–YODER, M.–RUNDLE, J. (eds.): *Earthquakes and multi-hazards around the pacific rim, Volume I.* Pageoph topical volumes Birkhäuser, Cham. https://doi.org/10.1007/978-3-319-71565-0_15

INTERNET SOURCE

NADERZADEH, A.–MADANI, R. (2012): *Time-predictable earthquake modeling on a segment of the Zagros mountain front Fault (pol-e-Zahab region) West Iran* 15 WCEE Lisboa. https://www.iitk.ac.in/nicee/wcee/article/WCEE2012_1445.pdf (downloaded: February 2024)